NUMERICAL MODELING AND PARAMETRIC STUDY OF A WET AIR FLOW BETWEEN PARALLEL PLATES

Ana C. O. de Paula
Kamal A. R. Ismail
ana.carolina@fem.unicamp.br
kamal@fem.unicamp.br
University of Campinas, Faculty of Mechanical Engineering, Department of Energy, Rua Mendeleyev, 200, Cidade Universitária “Zeferino Vaz”, Postal Code 13083-860, Campinas – SP, Brazil.

Abstract. *The present paper investigates numerically heat transfer and fluid flow by binary natural convection in a cavity filled with air and water vapor, and analyzes the effects of varying inclination and aspect ratio on Nusselt number, Sherwood number and condensation rate. The cavity has the top and bottom sides inclined and subject to temperature and concentration gradients, while the vertical walls are adiabatic. Water vapor is considered at the saturation state. The governing equations are conservation of mass, energy, momentum and concentration. These equations are discretized by the finite volume method. The conservation equations are coupled, and their solutions are based on the algorithm SIMPLE. Velocity, temperature and concentration fields are obtained for a Rayleigh number range where laminar flow prevails, and for different cavity inclination angles and aspect ratios. Results show that for high Rayleigh number, an increase in cavity inclination causes Nusselt number, Sherwood number and condensation rate increase. When aspect ratio is decreased, Nusselt and Sherwood numbers decreases, however, condensation rate at the cold wall increases due to the increment of the condensation area. From the results, a cavity of good thermal performance has 60 degrees inclination and aspect ratio of 1/12 when thermal Rayleigh number (Ra_T) is 10^6.*

Keywords: *Binary natural convection, Finite volume method, Algorithm SIMPLE, Inclined cavity, Condensation rate*

1 INTRODUCTION

Natural convection is a phenomenon that takes place in many engineering processes, which enhanced numerical and experimental investigations. One of the first numerical studies in natural convection field was elaborated by Vahl Davis (1983). In his work, a numerical solution was obtained for a cavity at thermal Rayleigh number varying from 10^3 to 10^6. He considered a square cavity where the vertical walls were at different levels of temperature. His results are benchmark and have been used for validation of other numerical studies.

When high thermal Rayleigh number range is desired, the classical Boussinesq 2-D equations becomes unsteady, especially for values close to 10^8. Le Quéré (1991) proposed a solution using pseudo-spectral discretization to provide accurate solutions for values of Rayleigh between 10^7 and 10^8.

Many engineering applications involve not only fluid motion due to temperature difference, but also due to gradients of other scalar quantities. This phenomenon is called binary natural convection and occurs in refrigeration towers, pollutants dispersion applications, drying processes and solar distillation.

Béghein et al. (1992) published a numerical study considering double-diffusion in a closed square cavity filled with air and pollutants. In his work, thermal and solutal buoyancy forces were studied and their effect compared through Nusselt and Sherwood numbers. If flow in the cavity is solute dominated, the concentration boundary layer is thicker than thermal boundary layer. Weaver and Viskanta (1992) elaborated a numerical-experimental study that illustrates thermal and solutal forces. In their study it was verified the change in flow direction when buoyancy parameters were reversed in direction.

Most of available investigations consider Boussinesq approximation and constant thermophysical properties in the domain to represent natural convection effects. This approximation is reasonable when temperature difference in the domain is not high enough to cause significant properties changes. Chenoweth and Paolucci (1986), however, points out in their study that, for large temperature differences, the flow becomes sensitive to property variations making an incompressible analysis unreasonable. In this case, Boussinesq limit is extrapolated and conservative equations strongly coupled to state equations and thermophysical properties. Seizai and Mohamad (2000) investigated a cubic cavity for opposing, horizontal, thermal and solutal gradients. It was found that secondary flow structures develop on the planes perpendicular to the main flow, especially for high Rayleigh number. Le Queré et al. (2005) presented results for a two-dimensional model with large temperature differences and low Mach number using “non-Boussinesq” approach.

Alvarado et al. (2008) studied a slender tilted cavity where natural convection and surface thermal radiation were considered. The authors concluded that total heat transfer changes when aspect ratio and tilt angle are varied. De Paula and Ismail (2017) published results for binary natural convection in an inclined cavity and concluded that Nusselt and Sherwood numbers peaks exist at the hot wall in the regions of high gradients of temperature, concentration and velocities.

This paper numerically investigates the effects of tilt angle and aspect ratio changes in a cavity where binary natural convection takes place. The cavity contains two horizontal adiabatic and impermeable walls and two vertical walls subject to temperature and species concentration gradient. The cavity performance is evaluated through heat and mass transfer parameters such as Nusselt and Sherwood numbers, and condensation rate. Temperature difference is considered low, thus, Boussinesq approach is applied along with constant thermophysical properties. Two species are considered in the domain: air and vapor.

2 ANALYSIS

The domain considered for analysis consists in a two-dimensional cavity, as shown in Fig. 1. Vertical walls are adiabatic and impermeable. Upper and bottom walls are at different levels of temperature and concentration, so fluid motion is generated. The temperature of bottom wall is slightly higher than upper wall. At the bottom, a liquid layer is present and saturated vapor is generated. At lower temperature wall, the new species (vapor) condenses out of the mixture inside the cavity.

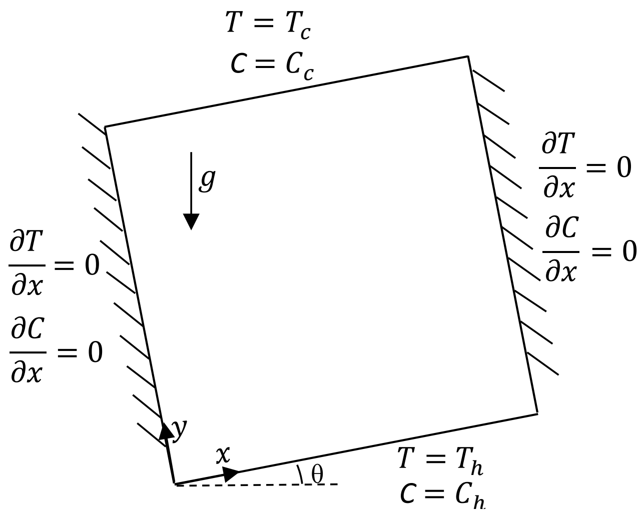

Figure 1. Cavity scheme

The representation of fluid dynamics, heat and mass transfer in the cavity is accomplished considering conservative equations. These equations are expressed in terms of differentials. The variables are the same as in pure convection problem, adding one additional quantity: concentration of vapor. Considering Cartesian coordinate system, the continuity equation is:

$$\frac{\partial \rho}{\partial t} + \frac{\partial (\rho u)}{\partial x} + \frac{\partial (\rho v)}{\partial y} = 0 . \tag{1}$$

where ρ corresponds the density of main species (air), u and v corresponds to velocities in x and y directions respectively in the local coordinate system. Momentum equations in x and y are:

$$-\frac{\partial p}{\partial x} + \mu\left(\frac{\partial^2 u}{\partial x^2} + \frac{\partial^2 u}{\partial y^2}\right) + \left(\rho - \rho_{ref}\right) g sin(\theta) = \frac{\partial (u\rho)}{\partial t} + \frac{\partial (\rho u \cdot u)}{\partial x} + \frac{\partial (\rho v \cdot u)}{\partial y} . \tag{2}$$

$$-\frac{\partial p}{\partial y}+\mu\left(\frac{\partial^2 v}{\partial x^2}+\frac{\partial^2 v}{\partial y^2}\right)+\left(\rho-\rho_{ref}\right)g\cos(\theta)=\frac{\partial(v\rho)}{\partial t}+\frac{\partial(\rho u\cdot v)}{\partial x}+\frac{\partial(\rho v\cdot v)}{\partial y}. \quad (3)$$

where p is the pressure acting in the corresponding control volume, ρ_{ref} is the reference density (density of air at T_{ref}), g is the gravitational acceleration, θ the cavity tilt angle and μ is the dynamic viscosity of air. Energy equation is:

$$\frac{k}{c_p}\left(\frac{\partial^2 T}{\partial x^2}+\frac{\partial^2 T}{\partial y^2}\right)=\frac{\partial(\rho T)}{\partial t}+\frac{\partial(\rho u\cdot T)}{\partial x}+\frac{\partial(\rho v\cdot T)}{\partial y}. \quad (4)$$

where k and c_p are the air thermal conductivity and specific heat respectively. The temperature is referenced by T. Species concentration equation is:

$$D_v\left(\frac{\partial^2 C_v}{\partial x^2}+\frac{\partial^2 C_v}{\partial y^2}\right)=\frac{\partial(C_v)}{\partial t}+\frac{\partial(u\cdot C_v)}{\partial x}+\frac{\partial(v\cdot C_v)}{\partial y}. \quad (5)$$

where D_v is the binary diffusive coefficient and C_v is the concentration of the second species (water vapor). Heat generation and chemical reactions have been neglected and the fluid is considered Newtonian. The reference temperature (T_{ref}) and concentration (C_{ref}) are given by (T_h + T_c)/2 and (C_h + C_c)/2 respectively, where T_h, C_h, T_c and C_c are the temperatures and concentrations at hot and cold wall. .The buoyancy term is evaluated by Boussinesq approximation:

$$\left(\rho-\rho_{ref}\right)=\rho\beta_T\left(T_{ref}-T\right)+\rho\beta_S\left(C_{ref}-C\right). \quad (6)$$

where β_T and β_S are the thermal and solutal expansion coefficients respectively. They are given by:

$$\beta_T=-\frac{1}{\rho}\left(\frac{\partial\rho}{\partial T}\right)_p=\frac{1}{T_{ref}}. \quad (7)$$

$$\beta_S=-\frac{1}{\rho}\left(\frac{\partial\rho}{\partial C}\right)_{p,T}=\frac{M_a-M_v}{C_{ref}M_v+C_aM_a}. \quad (8)$$

where M_a and M_v are the molecular weight of air and vapor respectively. The non-dimensional variables to the local system are considered:

$$T^*=\frac{T-T_c}{T_h-T_c}, x^*=\frac{x}{H}, y^*=\frac{y}{H}, u^*=\frac{uH}{\alpha}, v^*=\frac{vH}{\alpha}, C^*=\frac{C-C_c}{C_h-C_c}. \quad (9)$$

where H is the height of the cavity and L is the length. The thermal diffusive coefficient is represented by α. The cavity aspect ratio is defined:

Proceedings of the XXXVIII Iberian Latin-American Congress on Computational Methods in Engineering
P.O. Faria, R.H. Lopez, L.F.F. Miguel, W.J.S. Gomes, M. Noronha (Editores), ABMEC, Florianópolis, SC, Brazil, November 5-8, 2017.

$$A = H/L. \tag{10}$$

The temperature difference between hot and cold wall is defined by the non-dimensional temperature parameter $\in$:

$$\in = \left(T_h - T_c\right) / \left(T_h + T_c\right). \tag{11}$$

Thermal and solutal Rayleigh numbers are defined as:

$$Ra_T = \frac{g\beta_T\left(T_h - T_c\right)H^3}{\nu\alpha}. \tag{12}$$

$$Ra_S = \frac{g\beta_S\left(C_h - C_c\right)H^3}{\nu D_v}. \tag{13}$$

where ν is the kinematic viscosity of the main species (air). Prandtl and Lewis number are defined:

$$\Pr = \frac{\nu}{\alpha}. \tag{14}$$

$$Le = \frac{\alpha}{D_v}. \tag{15}$$

The local Nusselt and Sherwood numbers are:

$$Nu = uT^* - \frac{\partial T^*}{\partial y^*}. \tag{16}$$

$$Sh = Le\left(uC^* - \frac{1}{Le}\frac{\partial C^*}{\partial y^*}\right). \tag{17}$$

The buoyancy forces ratio is defined by the dimensionless parameter:

$$N = \frac{\beta_S \Delta C}{\beta_T \Delta T}. \tag{18}$$

Condensation rate can be obtained by the following relation:

$$\dot{m}_{ew} = \frac{\dot{q}_{ew}}{h_{fg}}. \tag{19}$$

where q_{ew} corresponds to the evaporative heat transfer rate and h_{fg} the latent heat of vaporization. The evaporative heat transfer rate can be calculated:

$$\dot{q}_{ew} = \left(\frac{h_{fg}}{c_p} \frac{M_w}{M_a} \frac{1}{P_T} \right) h_{cw} \left(P_h - P_c \right). \tag{20}$$

where h_{cw} is the evaporation heat transfer coefficient, P_h and P_c are the partial vapor pressure at hot and cold walls. Total condensation rate is obtained multiplying $\dot{m}_{ew}$ per condensable area:

$$\dot{M}_{ew} = \dot{m}_{ew} L. \tag{21}$$

where L is the cavity length. Coordinate z is a unit.

2.1 Boundary conditions

The domain consists of a square cavity in which natural convection takes place. The dimensions are $0 \leq x \leq L$ and $0 \leq y \leq H$. The considered tilt angle range is $15^{o} \leq \theta \leq 60^{o}$ and aspect ratio $1/12 \leq A \leq 1$. The reference temperature is taken T_{ref} = 300 K and non-dimensional temperature difference defined ϵ=0.1 (thus, Boussinesq approximation can be applied). Bottom and top walls are subject to T_h and T_c respectively:

$$T_h = T_{ref} \left(1 + \in \right). \tag{22}$$

$$T_c = T_{ref} \left(1 - \in \right). \tag{23}$$

Air and vapor are considered to be ideal gases. Vapor concentration at the walls of higher and lower temperatures can be obtained through the state equation for an ideal gas. Thus:

$$C_h = \frac{p_{sat}\left(T_h \right)}{\Re T_h}. \tag{24}$$

$$C_c = \frac{p_{sat}\left(T_c \right)}{\Re T_c}. \tag{25}$$

For adiabatic and impermeable vertical walls:

$$\frac{\partial T}{\partial y} = \frac{\partial C}{\partial y} = 0. \tag{26}$$

Since walls are fixed and there is no income of fluid through them, the conditions are valid:

$$u_{wall} = v_{wall} = 0\,. \tag{27}$$

Thermophysical properties considered in the domain are taken at the reference temperature:

$$\begin{aligned} &k = 2.63 \times 10^{-2} W / mK \\ &c_p = 1.007 \times 10^{3} J / kgK \\ &\rho = 1.1614 kg / m^3 \\ &\Pr = 0.71 \\ &D_v = 0.26 \times 10^{-4} m^2 / s \end{aligned} \quad . \tag{28}$$

3 NUMERICAL TREATMENT

Equations (1-5) are numerically discretized using finite volume method. Convection terms are approximated using upwind scheme while diffusive terms are approximated by central difference. Fully implicit scheme is used for time discretization. A SIMPLE (abbreviation for Semi-Implicit Method for Pressure-Linked Equations) algorithm was used to couple momentum and continuity equations, as presented by Patankar (1980). False transient formulation and variable under-relaxation were utilized to improve convergence. In the mentioned procedure, velocities are iteratively corrected. Other quantities fields (such as temperatures and concentrations) are calculated after velocities field is obtained. Temperatures and concentrations are calculated in a 80x80 main grid while velocities components are obtained in a staggered grid. Both grids are non-uniform and refined in the regions close to the walls. The following transformation function is used by Sengupta (2011) and is also used in this work:

$$x(\xi) = \frac{L}{2}\left[1 - \frac{\tanh(1-2\xi)}{\tan(\varphi)}\right]. \tag{29}$$

where ξ corresponds to the dimensionless node number and φ the stretching factor. The convergence of numerical algorithm is reached when the residues of conservation equations are less than 10^{-10}. The calculation procedure follows the steps presented in Fig. 2.

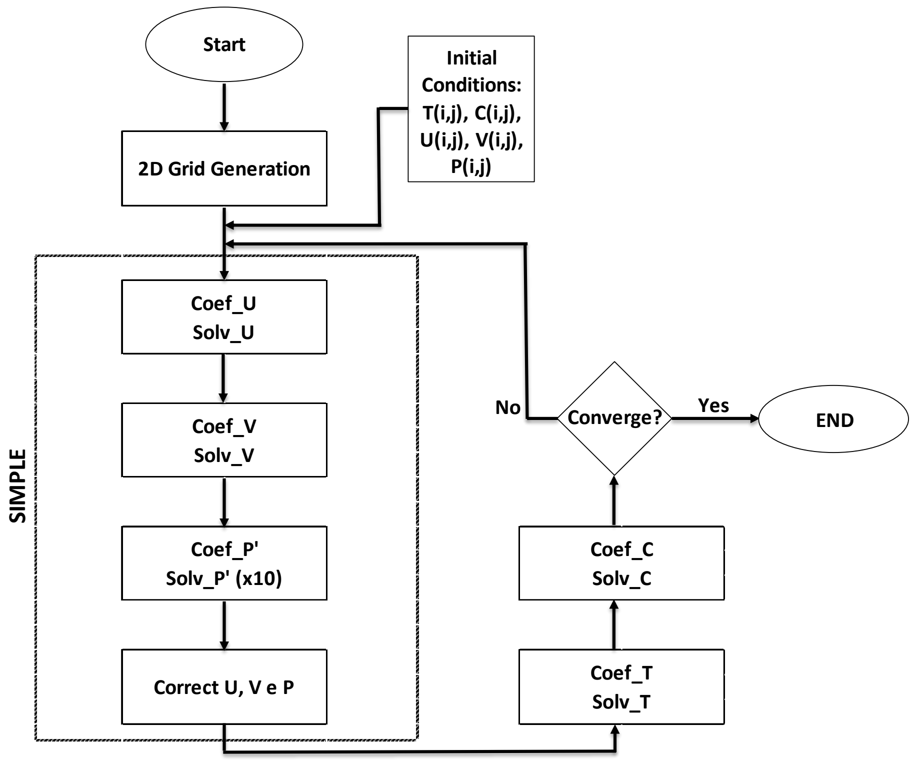

Figure 2. Numerical method for binary natural convection

3.1 Validation of numerical method

The validation of the numerical code for heat and mass transfer in a square situation was performed with the 2-D results published by Béghein et al. (1992) and the 3-D results published by Seizai and Mohamad (2000). Comparisons were performed to a differentially heated square cavity with species concentration difference between vertical walls. The mentioned authors used nonuniform 45x45 and 80x80x80 grids respectively for Le=1, Ra=10^7 and Pr=0,71 for different buoyancy ratios. The maximum difference in the Nusselt number obtained was less than 0.9%. Despite the dimension difference (2-D to 3-D model), the above conditions give a two-dimensional flow structure with negligible velocities in transverse planes. Results of the quantitative verification can be found in Table 1. The results for the qualitative comparison were performed for $Ra_T=10^4$ and $Ra_S=10^4$ and can be found on Fig. 3.

Table 1. Nusselt number along a vertical axis for $Ra_T = 10^7$ and N from -0.01 to 5.0

N Ra_S	-0.01 10^5	-0.2 2×10^6	-0.8 8×10^6	-1.5 1.5×10^7	-5.0 5×10^7
Béghein et al. (1992)	16.4	15.5	10.6	13.6	23.7
Seizai and Mohamad (2000)	16.27	15.37	10.51	13.54	23.55
Present work	16.36	15.45	10.61	13.62	23.66

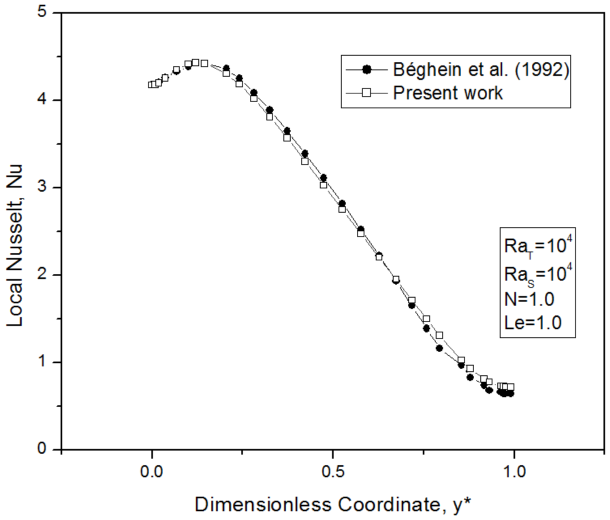

Figure 3. Validation of numerical code

4 RESULTS AND DISCUSSION

This section discusses the numerical solutions and results for heat and mass transfer inside a cavity subject to temperature and concentration gradients. All analysis is performed for thermal Rayleigh number between 10^3 and 10^6 in order of keeping the flow at laminar regime. The model applied is proper for low temperature gradient, thus properties can be considered constant. Top and bottom walls are subject to vapor concentration gradient. Water vapor is considered at saturate state and can be calculated through the state equation for ideal gases. In this work, the cavity height was varied so that it was possible to work in terms of the desired Rayleigh values. The cavity equivalent dimensions are presented in Table 2.

Table 2. Thermal Rayleigh numbers and equivalent cavity dimensions

Ra_T	H (m)	L(m)			
		A=1	A=1/4	A=1/8	A=1/12
10^3	0,009	0,009	0,036	0,072	0,108
10^4	0,021	0,021	0,084	0,168	0,252
10^5	0,045	0,045	0,180	0,360	0,540
10^6	0,097	0,097	0,388	0,776	1,164

4.1 Aspect ratio variation

Proceedings of the XXXVIII Iberian Latin-American Congress on Computational Methods in Engineering
P.O. Faria, R.H. Lopez, L.F.F. Miguel, W.J.S. Gomes, M. Noronha (Editores), ABMEC, Florianópolis, SC, Brazil, November 5-8, 2017.

This section treats a cavity of 15^o inclination. For each thermal Rayleigh number, the aspect ratio is varied from 1 to 1/12 and qualitative and quantitative comparison is made. The qualitative analysis is performed comparing fluid dynamics inside the cavity through temperature, species concentration and stream function contour lines. The quantitative analysis is accomplished through Nusselt and Sherwood numbers and condensation rate comparisons.

Figure 4 presents stream function contour lines inside the cavity for thermal Rayleigh numbers of 10^4 (left) and 10^6 (right) when aspect ratio is varied from 1 to 1/12. When the Rayleigh number increases from 10^4 to 10^6 streamlines become closer indicating large velocity gradients in the region close to the walls.

It can be seen that for $Ra_T = 10^4$, the increase in the aspect ratio results in the presence of multiple convection cells in the cavity. For A = 1 a single cell pattern is observed, while for A = 1/12, 7 convection cells are present. The lower the aspect ratio is, the higher are the quantities of convection cells. This effect occurs because the buoyancy forces are not great enough to maintain the flow in a single convection cell in the available cavity area. However, for higher Rayleigh number ($Ra_T = 10^6$) this multicellular pattern disappear due to the increase in buoyancy forces.

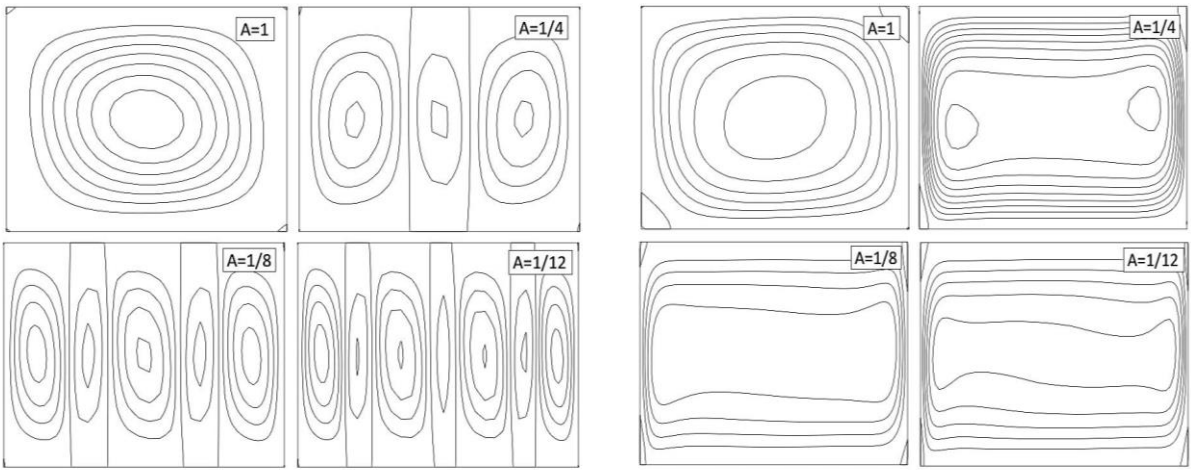

Figure 4. Streamlines for $Ra_T=10^4$ (left) and $Ra_T=10^6$ (right) for different aspect ratios

Figures 5 and 6 present temperature and water vapor concentration contour lines inside the cavity for Rayleigh numbers of 10^4 (left) and 10^6 (right) when aspect ratio is varied from 1 to 1/12. Due to the multicellular profile, it can be seen that for lower cavity buoyancy forces ($Ra_T = 10^4$), temperature and concentration contour lines are more parallel than for cavity with high buoyancy forces ($Ra_T = 10^6$). Also, temperature and concentration variations in the center region are smaller for high Rayleigh number, indicating homogeneity of these quantities in the center. The thermal and species concentration boundary layer become thinner in the region close to the horizontal walls, therefore, greater gradients are present in this region.

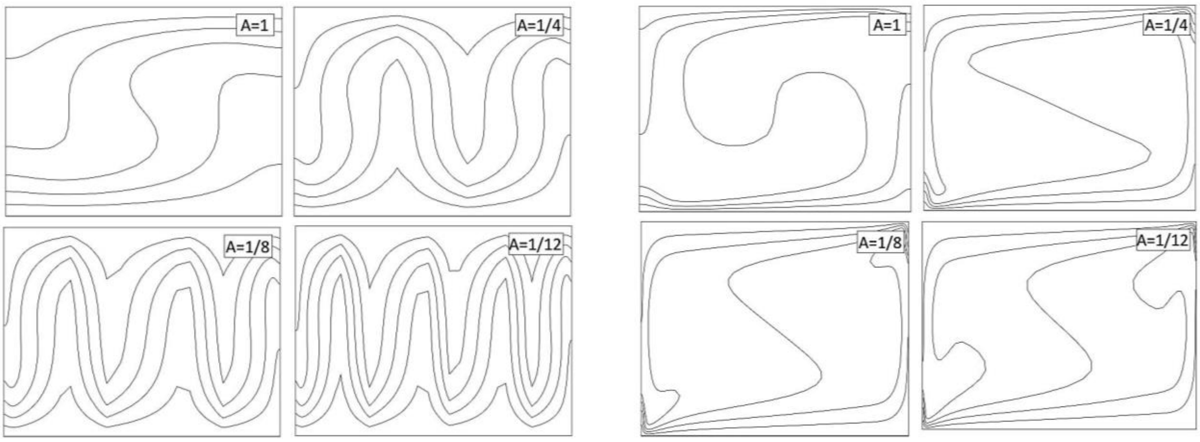

Figure 5. Temperature contour lines for $Ra_T=10^4$ (left) and $Ra_T=10^6$ (right) for different aspect ratios

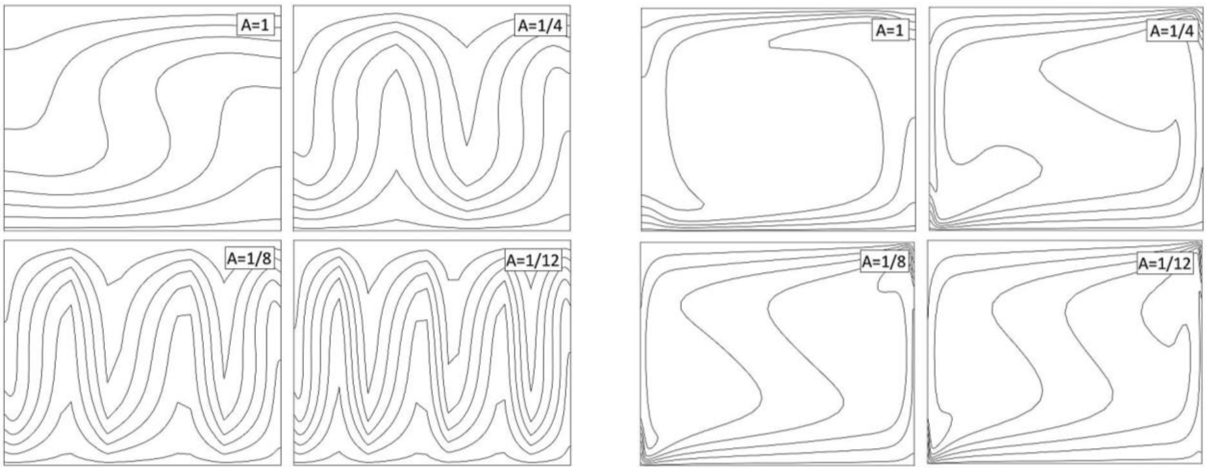

Figure 6. Concentration contour lines for $Ra_T=10^4$ (left) and $Ra_T=10^6$ (right) for different aspect ratios

Figure 7 shows the results for Nusselt and Sherwood numbers variations for different aspect ratios. Now, the analysis will be made for thermal Rayleigh number varying between 10^3 and 10^6. In general, it can be seen that the decrease in the aspect ratio causes a respective decrease in Nusselt and Sherwood numbers close to the hot wall. When a cavity has its aspect ratio reduced for the same values of Rayleigh number, a multicellular convection pattern emerges because more area is available for fluid flow. A multicellular pattern creates more shortcut paths for fluid flow, however, a certain quantity of fluid remains circulating at small velocity in the cavity core. Consequently, this pattern is not desired because heat and mass transfer from the hot to cold wall is reduced. For this reason, Nusselt and Sherwood numbers at the hot wall decrease when aspect ratio is decreased. In a single cellular pattern, contour lines are concentrated in the regions close to the walls. This effect enhances mass transfer from the hot to the cold wall.

Proceedings of the XXXVIII Iberian Latin-American Congress on Computational Methods in Engineering
P.O. Faria, R.H. Lopez, L.F.F. Miguel, W.J.S. Gomes, M. Noronha (Editores), ABMEC, Florianópolis, SC, Brazil, November 5-8, 2017.

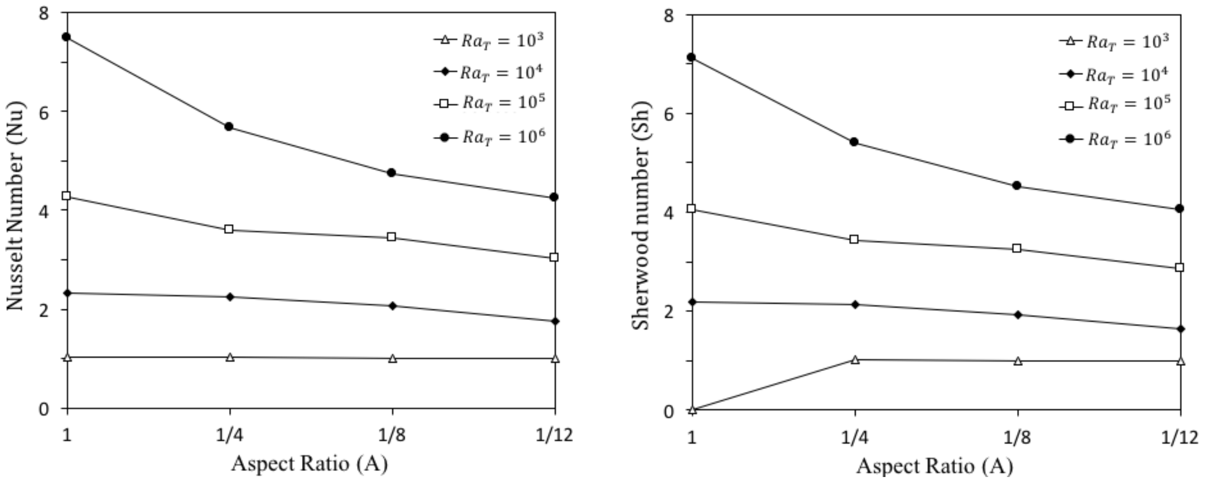

Figure 7. Nusselt number (left) and Sherwood number (right) at the hot plate for different aspect ratios

However, a different effect is observed for cavity total condensation rate. Despite Nusselt number and convection coefficient are directly related, when the cavity aspect ratio decreases, the condensation area increases, thus the total condensation rate increases. The highest total condensation rate is found for A = 1/12. The effects of variation between total condensation rate and aspect ratio can be found in Fig. 8, for different thermal Rayleigh numbers.

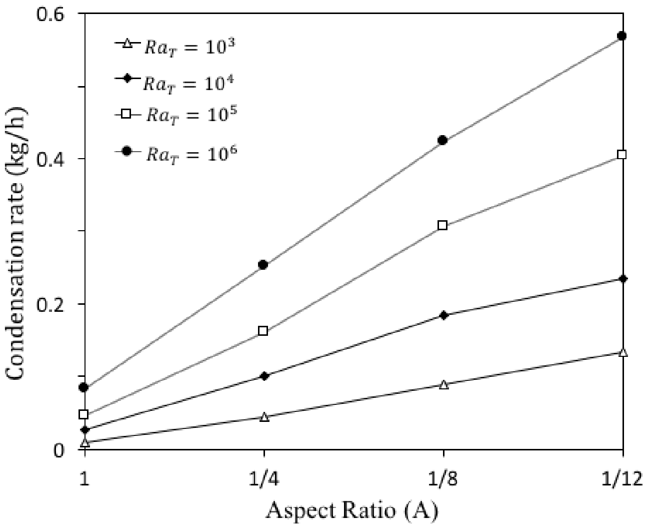

Figure 8. Total condensation rate for different aspect ratio

4.2 Tilt angle variation

In this section the tilt angle is varied from 15^o to 60^o for A=1/12 including comparison of the contour lines and heat transfer parameters.

Figure 9 presents stream function contour lines inside the cavity for thermal Rayleigh numbers of 10^4 (left) and 10^6 (right) when tilt angle is varied from 15^o to 60^o. For $Ra_T = 10^4$, for low tilt angles, a multicellular convection pattern can be observed. For θ=15^o inclination,

Proceedings of the XXXVIII Iberian Latin-American Congress on Computational Methods in Engineering
P.O. Faria, R.H. Lopez, L.F.F. Miguel, W.J.S. Gomes, M. Noronha (Editores), ABMEC, Florianópolis, SC, Brazil, November 5-8, 2017.

7 convection cells can be observed. For θ=30°, 3 convection cells can be observed and for $\theta \geq 45°$ a single cell pattern is present. Therefore, when the tilt angle increases, multicellular pattern tend to disappear. For Ra_T = 10^6, multicellular pattern is not observed, however, secondary cells can be found in the center of cavity for $\theta \geq 45°$.

Figures 10 and 11 present temperature and water vapor concentration contour lines inside the cavity for Rayleigh numbers of 10^4 and 10^6 when tilt angle is varied from 15° to 60°. It can be seen that the increase in cavity tilt angle decreases temperature and concentration variations in the core region of the cavity. When thermal Rayleigh number increases from 10^4 to 10^6, thermal and species concentration boundary layer become thinner in the region close to the horizontal walls indicating greater gradients of these quantities.

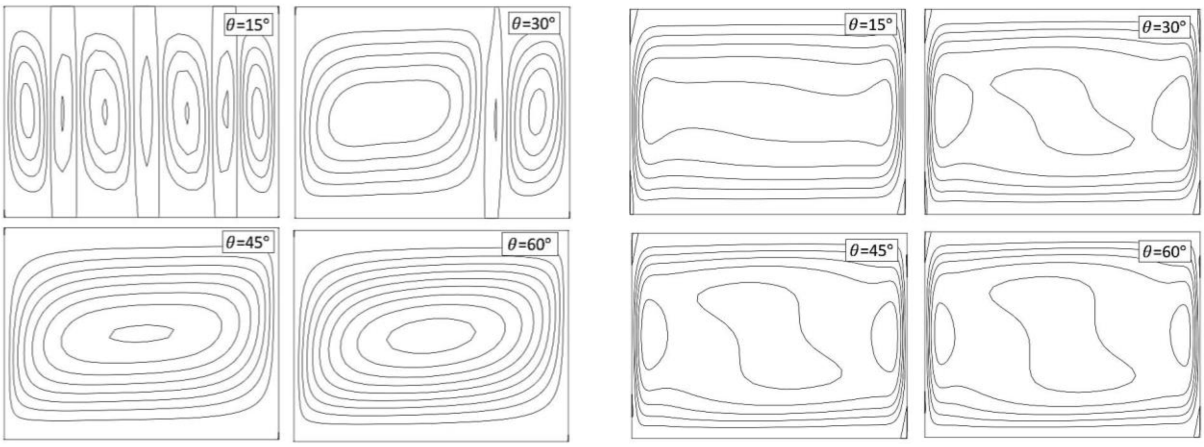

Figure 9. Streamlines for Ra_T=10^4 (left) and Ra_T=10^6 (right) for different tilt angles

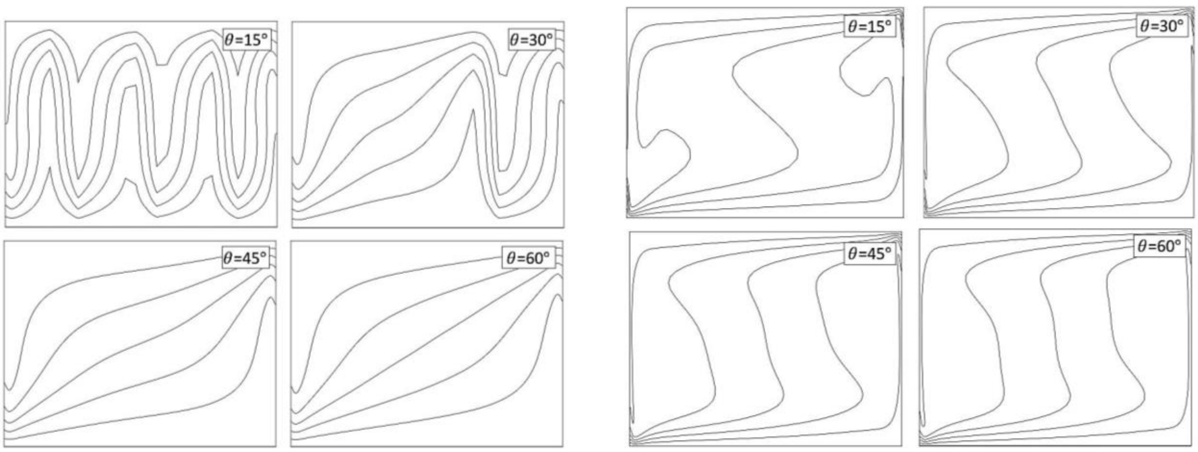

Figure 10. Temperature contour lines for Ra_T=10^4 (left) and Ra_T=10^6 (right) for different tilt angles

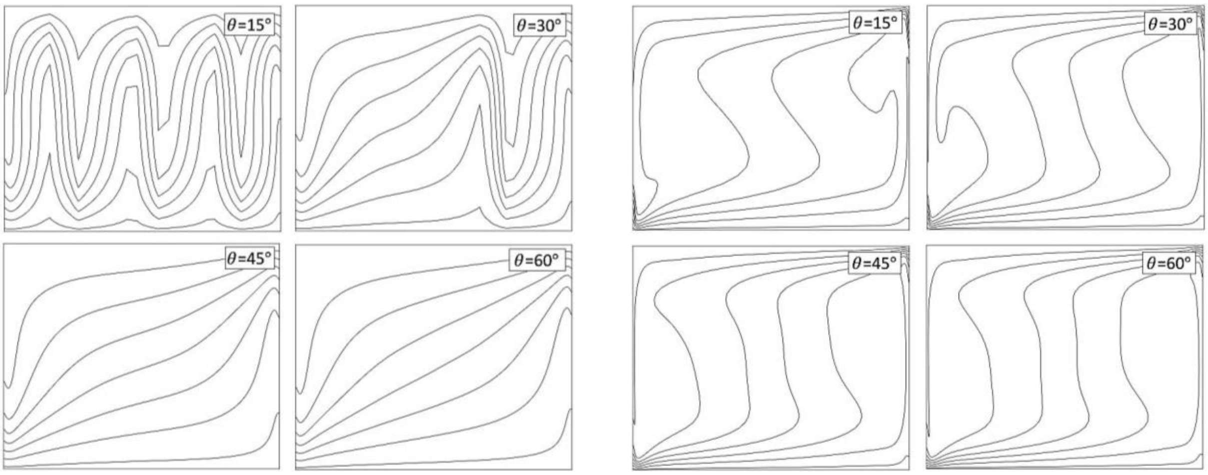

Figure 11. Concentration contour lines for Ra_T=10^4 (left) and Ra_T=10^6 (right) for different tilt angles

Figure 12 shows the results for Nusselt and Sherwood numbers variations for different tilt angles. These dimensionless parameters do not follow the same pattern as when the aspect ratio is varied. For $Ra_T = 10^6$ a single convection cell pattern can be observed for high or low aspect ratio, thus, the inclination in the cavity causes an increase in temperature and concentration gradients close to the walls. However, for lower thermal Rayleigh number, a multicellular convection pattern is present and an increase in tilt angle results in extinction of convection cells. This effect can be observed for the case where $Ra_T = 10^4$. The number of convection cells gradually decrease until one single cell pattern is present. Nusselt and Sherwood numbers gradually decrease when tilt angle varies in the range of $15^o \geq \theta \leq 45^o$ due to the change in flow pattern from a multicellular structure to a single cell structure. Once a single cell pattern is achieved, the increase in the inclination angle has the effect of increasing temperature and concentration gradients in the region close to the walls.

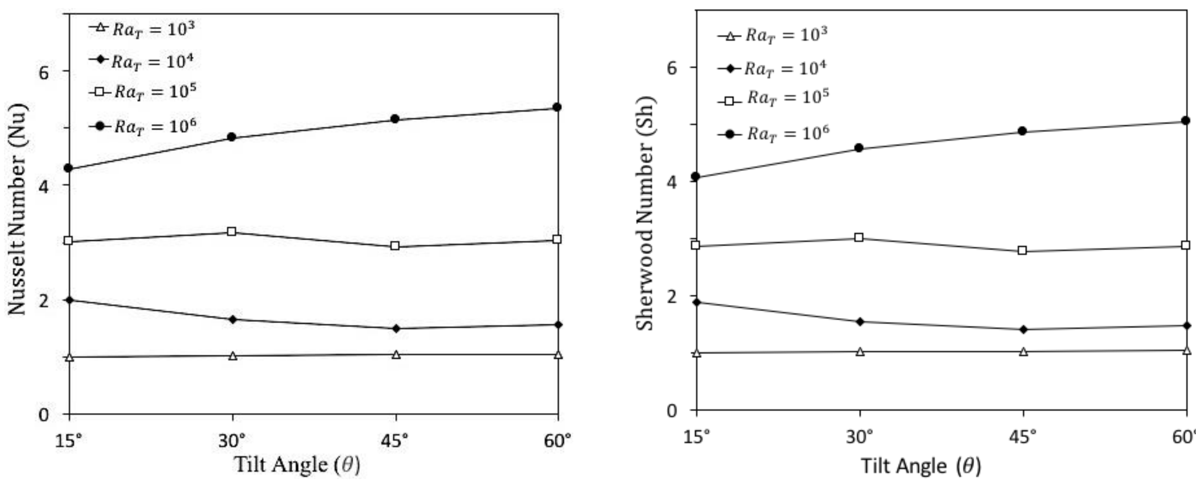

Figure 12. Nusselt number (left) and Sherwood number (right) at the hot plate for different tilt angles

A similar behavior is found for cavity total condensation rate, once there is no change in aspect ratio and Nusselt number and condensation rate are directly related. The effects of variation between total condensation rate and tilt angle can be found on Fig. 13. The biggest total condensation rate was found $Ra_T = 10^6$ for $\theta = 60^o$, where a single convection cell is present.

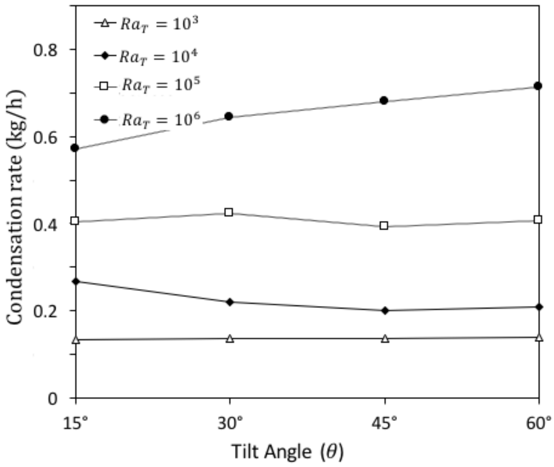

Figure 13. Total condensation rate for different tilt angles

5 CONCLUSIONS

Conservation of mass, momentum, energy and species concentration of an inclined cavity were numerically studied for laminar convection considering the Rayleigh range between 10^3 and 10^6, tilt angle between 15^o and 60^o and aspect ratio between 1 and 1/12. Results indicate that aspect ratio and cavity tilt angle variation cause changes in the fluid dynamics and heat transfer inside the cavity. A multicellular convection pattern exists for small aspect ratios and small thermal Rayleigh number. For small thermal Rayleigh number, when aspect ratio is increased the quantity of convection cells inside the cavity also increases. Once a certain quantity of fluid remains circulating at low velocity in the center of the cavity, heat and mass transfer between hot and cold wall is decreased. Consequently, Nusselt and Sheerwood numbers at the hot wall decrease when aspect ratio is increased. Total condensation rate increases because there is more condensation area available.

On the other hand, the increase in cavity tilt angle results in the extinction of multicellular pattern. Thus, Nusselt and Sherwood numbers gradually decrease for small tilt angle due to the change in flow pattern from multicellular to single cell. Once a single cell pattern is achieved, the increase in tilt angle causes increase in Nusselt and Sherwood numbers and condensation rate. Finally, a cavity of good thermal performance has $Ra_T = 10^6$, aspect ratio of 1/12 (for increased condensation area) and tilt angle of 60^o (because of desired single cell pattern).

Acknowledgements

Authors wish to thank CAPES (Coordenação de Aperfeiçoamento de Pessoal de Nível Superior) for graduate scholarship to the first author and CNPQ (Conselho Nacional de Desenvolvimento Científico e Tecnológico) for PQ Research Grant to the second author.

REFERENCES

Alvarado, R., Xamán, J., Hinojosa, J., & Álvarez, G., 2008, Interaction between natural convection and surface thermal radiation in tilted slender cavities. *International Journal of Thermal Sciences*, vol. 47, pp. 355-368.

Béghein, C., Haghighat, F., & Allard F., 1992, Numerical study of double-diffusive natural convection in a square cavity, *International Journal of Heat and Mass Transfer*, vol. 35, pp. 833-846.

Chenoweth, D. R., & Paollucci, S., 1986, Natural convection in an enclosed vertical air layer with large horizontal temperature, *Journal of Fluid Mechanics*, vol. 169, pp. 173-210.

De Paula, A. C. O., & Ismail, K. A. R., 2017, Analytical modeling and numerical solution of a simple solar still, *Proceedings of 13th International Conference on Heat Transfer, Fluid Mechanics and Thermodynamics*, pp. 452-457

Le Quéré, P., 1991, Accurate solutions to the square differentially heated cavity at high rayleigh number, *Computer Fluids*, vol. 20, pp. 29-41.

Le Quéré, P., Weisman, C., Paillère, H., Vierendeels, J., Dick, E., Becker, R., Braack, M., & Locke J., 2005, Modeling of natural convection flows with large temperature differences: a benchmark problem for low mach number solvers. part 1., *ESAIM: Mathematical Modeling and Numerical Analysis*, 2005, pp. 609-616.

Patankar, S., 1980, Numerical heat transfer and fluid flow, CRC Press.

Seizai, I., & Mohamad, A., 2000, Double diffusive convection in a cubic enclosure with opposing temperature and concentration gradient, *Physics of Fluids*, vol. 12, n. 9, pp. 2210-2223.

Sengupta, T. K., Bhaumik, S., & Shameen, U., 2011, A new compact difference scheme for second derivative in non-uniform grid expressed in self-adjoint form, *Journal of Computational Physics*, vol. 230, pp. 1822-1848.

Vahl Davis, G., 1983, Natural convection of air in a square cavity: a bench mark numerical solution. *International Journal for Numerical Methods in Fluid*, vol. 3, pp. 249-264.

Weaver, J. A., & Viskanta, R., 1992, Natural convection in binary gases driven by combined horizontal thermal and vertical solutal gradients, *Experimental Thermal and Fluid Science*, vol. 5, pp. 57-68.